

Electronic Supplementary Information

Synthesis of ligand-functionalized water-soluble [^{18}F]YF₃ nanoparticles for PET imaging

Liqin Xiong,^{*abc} Bin Shen,^a Deepak Behera,^a Sanjiv S. Gambhir,^a Frederick Chin,^a Jianghong Rao^{*a}

^a *Stanford Molecular Imaging Program (MIPS), Departments of Radiology and Chemistry, Stanford University, Stanford, CA 94305-5484, USA. E-mail: jrao@stanford.edu*

^b *School of Biomedical Engineering, Shanghai Jiao Tong University, Shanghai, 200030, P. R. China. E-mail: xiongliqin@sjtu.edu.cn*

^c *Department of Nuclear Medicine, Ruijin Hospital, Shanghai Jiao Tong University School of Medicine, Shanghai, 200025, P. R. China*

Table of Contents

1. Experimental section

1.1 Materials

1.2 Preparation of YF₃ nanoparticles

1.3 Preparation of doxorubicin (DOX) linked YF₃ nanoparticles

1.4 Characterization of YF₃ nanoparticles

1.5 Preparation of [^{18}F]YF₃ nanoparticles

1.6 Cell culture and cytotoxicity assay

1.7 Cell uptake analysis

1.8 *In vivo* lymph node microPET/CT imaging

2. Supporting figures

Fig. S1. The energy-dispersive X-ray analysis (EDXA) pattern confirmed the presence of Y, F, O and N in the FA-YF₃ samples.

Fig. S2. Transmission electron microscopy (TEM) images of the DOX-FA-YF₃ nanoparticles.

Fig. S3. Dynamic light scattering (DLS) measurement of YF₃ nanoparticles in water by lognormal size distribution.

Fig. S4. The UV-Vis absorbance spectra of the free folate and synthesized samples, and Job's plot of UV-Vis absorption (at $\lambda=281$ nm) vs folate concentration.

Fig. S5. The UV-Vis absorbance spectra of the free DOX and synthesized samples, and Job's plot of UV-Vis absorption (at $\lambda=478$ nm) vs DOX concentration.

Fig. S6. ^{18}F labeling yield of synthesized YF₃ nanoparticles.

Fig. S7. Stability of [^{18}F]YF₃ nanoparticles in the mouse and human serum.

Fig. S8. Lymph node imaging of rats injected with [^{18}F]YF₃ nanoparticles at the front foot pads.

Fig. S9. Lymph node imaging of rats injected with [^{18}F]YF₃ nanoparticles at the rear foot pads.

1. Experimental section

1.1 Materials

Ammonium fluoride, Yttrium(III) chloride hexahydrate, doxorubicin hydrochloride, citric acid, folate, and the other chemicals were purchased from Sigma Aldrich, Inc. and used without purification.

1.2 Preparation of YF_3 nanoparticles

In a typical synthesis, a solution of 1 mmol of citric acid in 3.5 mL of distilled water was adjusted with sodium hydroxide to pH 6~7 and heated to 75 °C. Next, folate (0.1 mmol) was added until the mixture became clear. This was followed by the addition of 0.12 mmol $YCl_3 \cdot 6H_2O$ in 0.2 mL of distilled water and 11 mg of NH_4F (0.3 mmol) in 0.4 mL of distilled water consecutively. After stirring for 0.5 h, the nanoparticles were precipitated with 5 mL of ethanol and isolated with centrifuge at 14,000 rpm for 15 min. The supernatant was poured off, and the residual supernatant was subsequently washed with ethanol and distilled water three times.

The folate groups on the surface of the FA- YF_3 nanoparticles were quantified by measuring the UV absorption of the FA- YF_3 nanoparticles and subtracting the UV absorption of the Cit- YF_3 nanoparticles at $\lambda=281$ nm. To synthesize Cit- YF_3 nanoparticles, the procedure was repeated without folate. To synthesize PEG- YF_3 nanoparticles, substitute Fmoc-PEG₂₀₀₀-COOH (28 mg) linkage in place of folate.

1.3 Preparation of doxorubicin (DOX) linked YF_3 nanoparticles

Aliquots of free DOX in water (0.3 mg in 0.4 mL) were added into an aqueous solution of Cit- YF_3 or FA- YF_3 (~3 mg, 0.1 mL), and the mixtures were stirred at room temperature for 24 h. After centrifugation (14,000 rpm for 30 min), the precipitate was washed with ethanol and centrifuged. The washing cycle was repeated until the supernatant became colorless. All supernatants collected were pooled together, and the amount of free DOX in the supernatant was determined by spectrophotometry at 478 nm.

1.4 Characterization of YF_3 nanoparticles

The size and morphology of the nanoparticles were investigated using Transmission Electron Microscope (TEM) (FEI Tecnai G2 F20 X-TWIN, 200 kV). TEM samples were prepared by dripping the nanoparticle solution onto a carbon-supported copper grid and drying it at room temperature before observation. Energy-dispersive X-ray analysis (EDXA) of the samples was also performed during TEM measurements. The hydrodynamic size of the nanoparticles was also measured in aqueous solution using a Dynamic Light Scattering (DLS) instrument (Brookhaven 90 Plus Nanoparticle Size Analyzer). The absorption spectra were recorded on an Agilent 8453 UV-Vis spectrometer.

1.5 Preparation of [^{18}F] YF_3 nanoparticles

In a typical synthesis, ^{18}F -fluoride (~0.3 mCi/11 MBq)- K_2CO_3 (5 μ g) solution (100 μ L) was mixed with nanoparticle solution (100 μ L) via vortexing and incubated at room temperature within 10 min. Free ^{18}F -fluoride was removed from the nanoparticles by centrifugation. The stability of [^{18}F] YF_3 nanoparticles (1 mg, 260 μ Ci/9.6 MBq) were tested

by incubation with mouse serum or human serum (1:1, v:v) at 37 °C for 0.5, 1, 2, 4, 6h, respectively. Free ^{18}F -fluoride was removed from the nanoparticles by centrifugation.

1.6 Cell culture and cytotoxicity assay

PYMT and MDA-MB-468 cell lines were grown in DMEM supplemented with 10% FBS. Cultures were maintained at 37 °C under a humidified atmosphere containing 5% CO_2 .

The *in vitro* cytotoxicity was measured using the methyl thiazolyl tetrazolium (MTT) assay in MDA-MB-468 cell line. Cells growing in log phase were seeded into a 96-well cell-culture plate at 1×10^4 /well and then incubated for 24 h at 37 °C under 5% CO_2 . Particles or free DOX (100 μL /well) at different concentrations were added to the wells of the treatment group, and 100 μL /well DMEM to the negative control group, respectively. The cells were incubated for 24 h at 37 °C under 5% CO_2 . Subsequently, 10 μL of MTT (5 mg/mL) was added to each well of the 96 well plate and incubated for an additional 4 h at 37 °C under 5% CO_2 . After the addition of DMSO (200 μL /well), the assay plate was allowed to shake at room temperature for 20 min. A Tecan microplate reader was used to measure the OD570 (A value) of each well with background subtraction at 690 nm. The following formula was used to calculate the viability of cell growth:

cell viability (%) = (mean of Absorbance value of treatment group / mean of Absorbance value of control) · 100.

1.7 Cell uptake analysis

Cell uptake studies were performed with the adherent PYMT (high folate receptor expression) and MDA-MB-468 (low folate receptor expression) cells. Cells growing in log phase were seeded into a 12-well cell-culture plate at a density of 1×10^4 /well and then incubated for 24 h at 37 °C under 5% CO_2 . [^{18}F]YF₃ (100 μL /well) was added to the wells of the treatment group. The cells were incubated with at 37 °C under 5% CO_2 for 45 min, 1 h, and 2 h, respectively. The radioactivity was evaluated using a Capintec PET Dose Calibrator.

1.8 *In vivo* lymph node microPET/CT imaging

Sprague-Dawley rats (Charles Rivers) were anesthetized with 3% isoflurane, and intracutaneous injections of ~50 μL of [^{18}F]YF₃ (~50 μCi /1.85 MBq) were administrated into the front or rear foot pads. *In vivo* lymph node imaging was carried out on a microPET/CT system (Siemens-Inveon). The PET imaging was acquired directly following a CT scan of approximately 15 min. A dynamic PET scan was performed from 15 to 45 min, and a 10 min PET static scan was performed at 1 h post-injection. Reconstructed CT and PET images were fused and analyzed using Inveon Research Workplace (IRW) software.

2. Supporting Figures

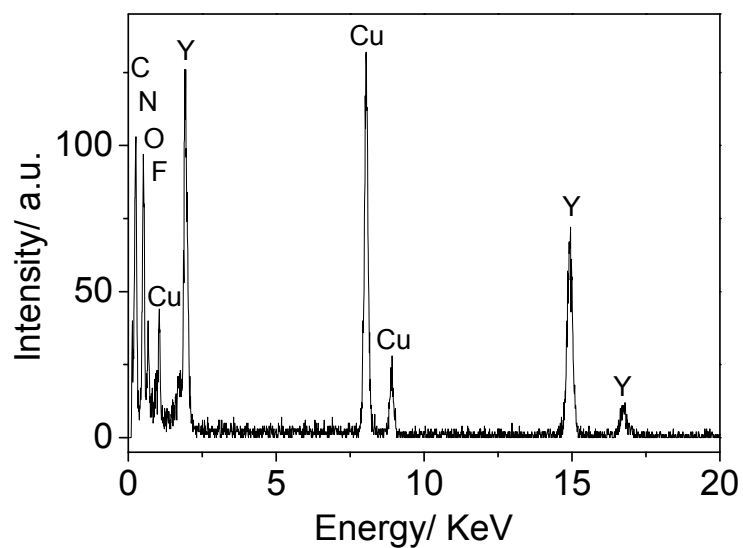


Fig. S1 The energy-dispersive X-ray analysis (EDXA) pattern confirmed the presence of Y, F, O and N in the FA-YF₃ samples.

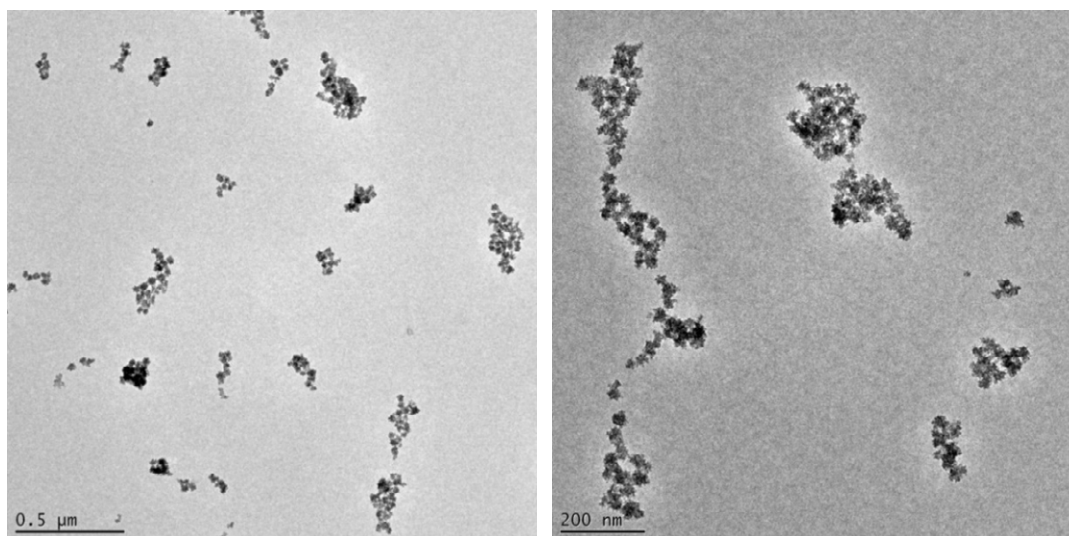


Fig. S2 Transmission electron microscopy (TEM) images of the DOX-FA-YF₃ nanoparticles.

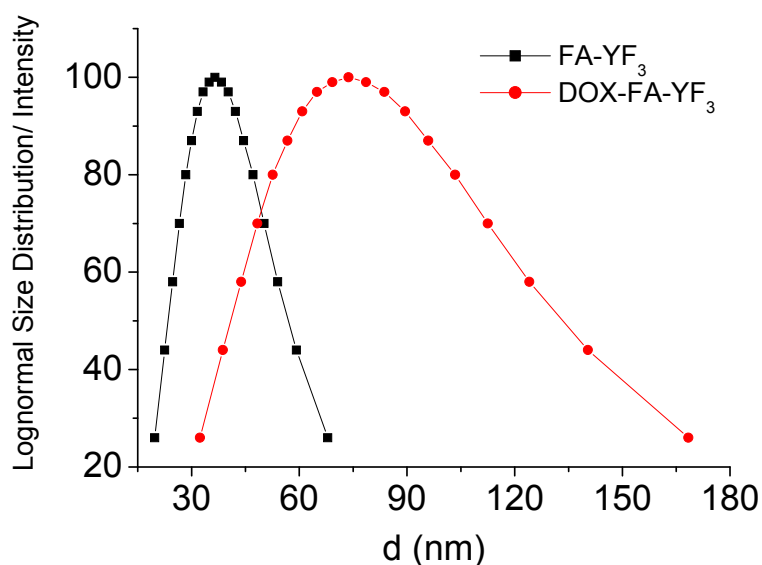


Fig. S3 Dynamic light scattering (DLS) measurement of YF₃ nanoparticles in water by lognormal size distribution.

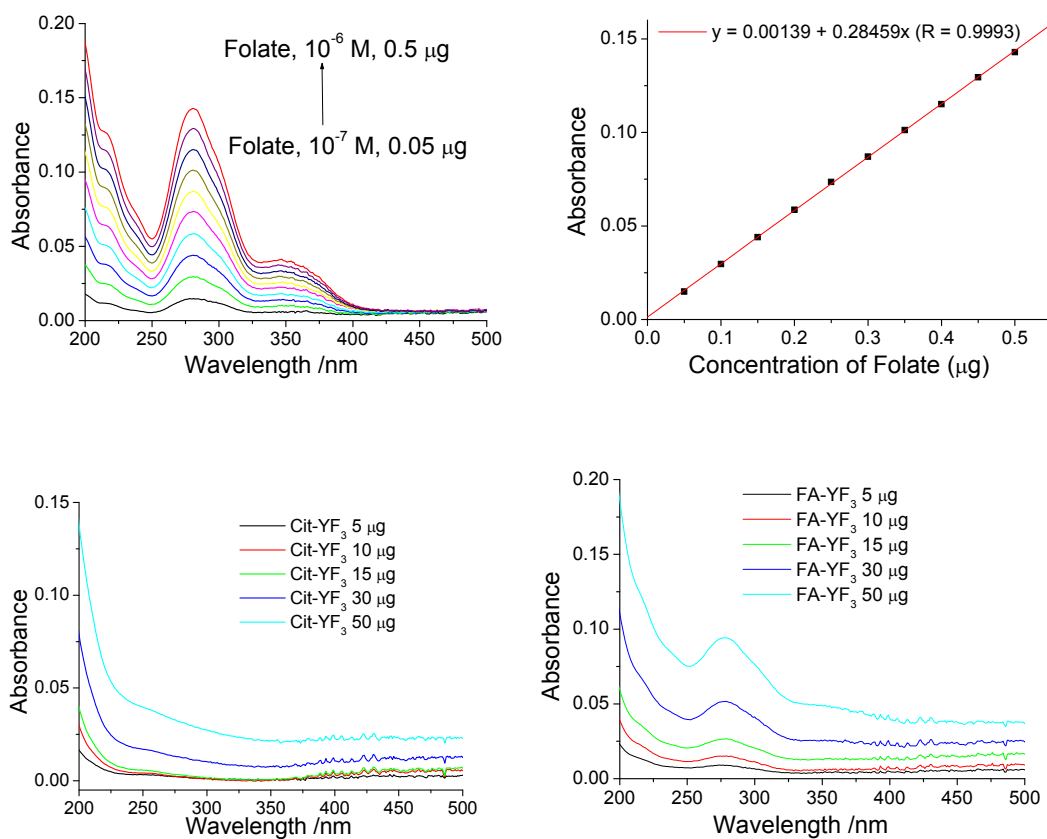


Fig. S4 The UV-Vis absorbance spectra of the free folate and synthesized samples, and Job's plot of UV-Vis absorption (at $\lambda=281$ nm) vs folate concentration.

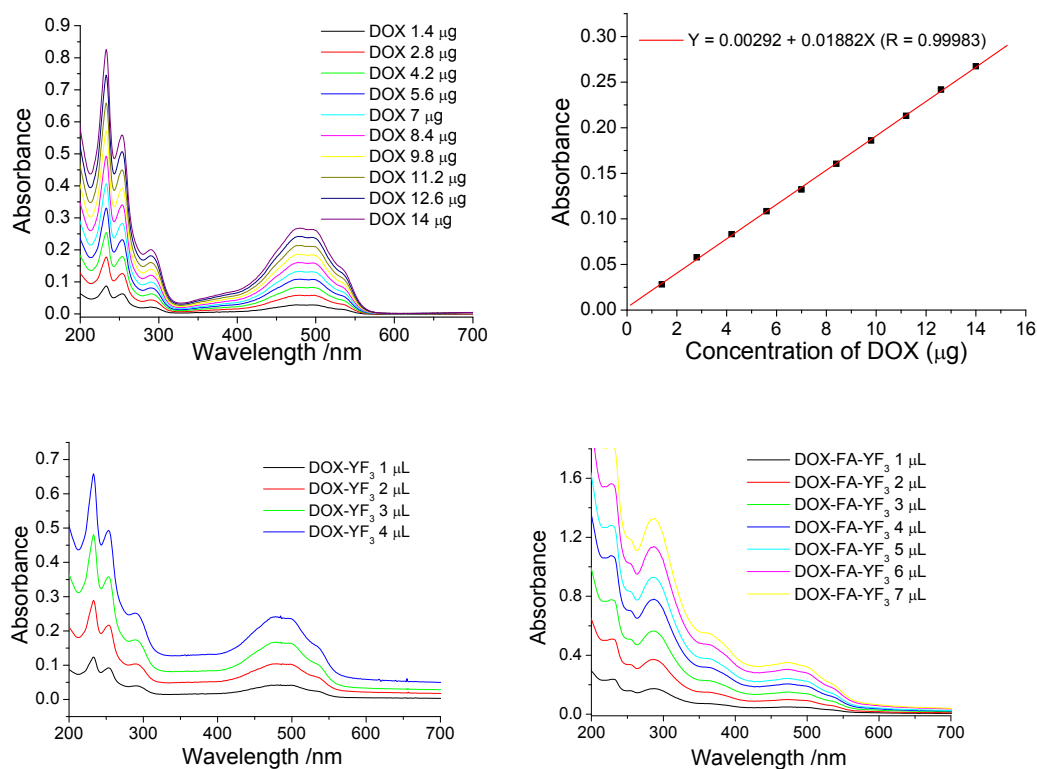


Fig. S5 The UV-Vis absorbance spectra of the free DOX and synthesized samples, and Job's plot of UV-Vis absorption (at $\lambda=478$ nm) vs DOX concentration.

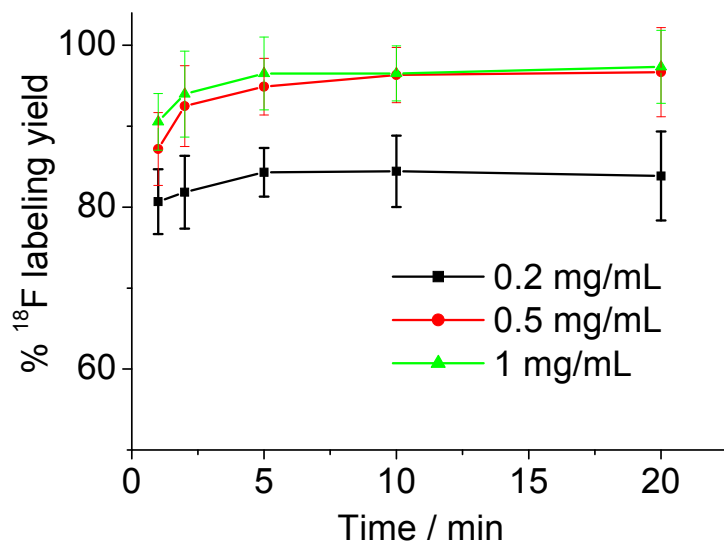


Fig. S6 ¹⁸F labeling yields of synthesized YF₃ nanoparticles at different reaction time and concentrations.

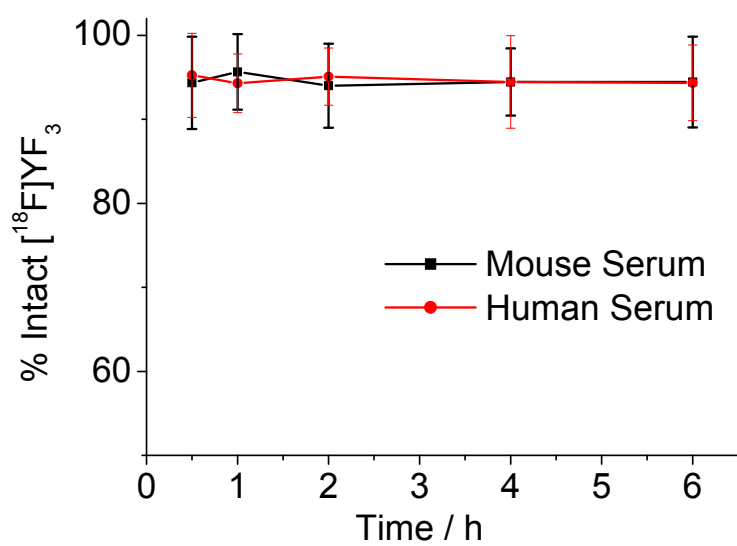


Fig. S7 Stability of $[^{18}\text{F}]\text{YF}_3$ nanoparticles in the mouse and human serum.



Fig. S8 Lymph node imaging of rats injected with $[^{18}\text{F}]\text{YF}_3$ nanoparticles at the front foot pads.



Fig. S9 Lymph node imaging of rats injected with [^{18}F]YF₃ nanoparticles at the rear foot pads.